Simulation of the bulk and surface properties of amorphous hydrogenated silicon deposited from silane plasmas

Michael J. McCaughey and Mark J. Kushner
Department of Electrical and Computer Engineering, Gaseous Electronics Laboratory, 607 East Healey, Champaign, Illinois 61820

(Received 12 August 1988; accepted for publication 9 September 1988)

A Monte Carlo simulation for the growth of amorphous hydrogenated silicon (*a*-Si:H) thin films by plasma enhanced chemical vapor deposition is presented. The goal of the model is to predict the bulk and surface properties of films (e.g., hydrogen content, deposition rate, buried hydride/dihydride ratios, porosity, and surface roughness) having thicknesses of $\lesssim 2000$ Å. The effects on the film properties of the composition of the radical flux incident on the surface are examined. Film properties were found to be critically dependent on the ratio of SiH_3/SiH_2 in the radical flux. High values for this ratio results in film properties resembling chemical vapor deposition. Film properties obtained with small values resemble physical vapor deposition. Rough films (roughness $>$ 10's of Å) accordingly result from radical fluxes having high SiH_2 fractions. We find that surface roughness and hydrogen fraction increase with increasing growth rate and increasing film thickness, though thin films ($<$ 10's of layers) have large hydrogen fractions due to there being a hydrogen rich surface layer with a thickness approximately equal to the surface roughness. We also find a correlation between porosity (subsurface voids) and hydrogen fraction, implying that the inner surfaces of voids are lined with $\equiv$Si—H configurations. In simulating films grown from Ar/SiH_4 gas mixtures, we find that a decrease in the SiH_3/SiH_2 ratio in the radical flux, and an increase in the ion/radical ratio incident on the surface are largely responsible for the degradation of film properties observed with decreasing silane fraction.

I. INTRODUCTION

Thin films of hydrogenated amorphous silicon (*a*-Si:H) fabricated by plasma enhanced chemical vapor deposition (PECVD) are valuable materials for the manufacture of thin-film transistors, direct-line contact sensors, xerographic materials, and solar cells.[1–4] The efforts of many researchers have resulted in a generally accepted working theory that device quality films [photoconductivity $> 10^{-5}$ $(\Omega\ cm)^{-1}$, low surface roughness, hydride/dihydride ratio > 1, spin density $\lesssim 10^{16}\ cm^{-3}$] are obtained from pure silane plasmas having radical fluxes incident on the substrate composed dominantly of silyl (SiH_3). The mechanisms responsible for this behavior were proposed by Gallagher.[5] He observed that silyl cannot directly insert into hydrogen passivated ($\equiv$Si—H) silicon bonds on the surface and as a result they are highly mobile in the adsorbed state. The residence time and sticking coefficient of these radicals then depends on the generation of dangling bonds on the surface by ion bombardment or etching reactions. The diffusive motion of these adsorbed radicals, filling in surface roughness, results in smooth films. Plasma conditions resulting in large fractions of silylene (SiH_2) in the radical flux, which can directly insert into passivated surface sites, or conditions which result in a high rate of activating surface sites by removing passivating H atoms, result in rougher poorer quality films.

In simulating the deposition of thin films of *a*-Si:H by PECVD one desires to predict physical and processing parameters such as growth rate, hydrogen fraction, hydride/dihydride ratio, local bond structure (Si—Si and Si—H bond angles), surface roughness, and porosity. An extension of this predictive capability would be to relate these physical parameters to electronic properties of the material, either on an *ab initio* or semiempirical basis. Although the qualitative description of film growth described above is logical, there are few, if any, quantitative models for film growth which can predict these properties based on the cited mechanisms. In a similar fashion, many models and descriptions of the plasma kinetics of silane discharges have been presented,[6–9] however few have correlated plasma properties to film characteristics. To date, Gleason *et al.*[10] have presented the most complete physical model of film growth based on first principles simulation techniques. Their model is capable of predicting bond angles, hydride ratios, hydrogen fraction, and local order. Their work, though, did not address thick films having many hundreds of layers. Therefore, bulk properties such as surface roughness and porosity were not predicted.

In this paper, we present a Monte Carlo simulation for the deposition of a-Si:H from silane glow discharges and we relate plasma properties (in the form of radical and ion fluxes to the substrate) to bulk and surface characteristics of the film. As described below, we do not address the issue of short-range order (e.g., bond angles) as discussed by Gleason *et al.*,[10] though, we do address bulk film properties such as porosity and surface roughness. By using computed radical fluxes from a companion model for the plasma chemistry of silane discharges,[6] a complete first-order model for the growth of a-Si:H films is presented.

The model presented here emphasizes the bulk properties of the film as opposed to local bond structure. The modeling techniques we use are capable of simulating the deposition of thick films exceeding many hundred of layers while

 0021-8979/89/010186-10$02.40

deemphasizing the details of the short-range order, particularly bond angles. This tradeoff is accomplished by assuming that the film is composed of a cubic lattice, where each lattice point may be occupied by either a silicon atom or a void. The use of the term lattice does not imply that there is any long-range order in the occupation probability of a site by a silicon atom. No assumptions are made concerning the coordination partners of each silicon atom. The amorphous character of the film results from the random distribution of coordination partners for each silicon atom in the lattice, and from the finite but random probability that a lattice point is occupied by either a silicon atom or a void.

In Sec. II, the Monte Carlo model for film growth is described in detail. Simulated properties of *a*-Si:H films (roughness, hydrogen content, porosity) deposited from silane plasmas are discussed in Sec. III using parametric radical fluxes. The simulation of PECVD *a*-Si:H films grown from Ar/SiH_4 gas mixtures is discussed in Sec. IV followed by concluding remarks in Sec. V.

II. DESCRIPTION OF THE MODEL

Our model for the growth of *a*-Si:H films uses Monte Carlo techniques to simulate the impingement and adsorption of gas phase radicals and ions on the surface of a growing film, as well as for the processes which occur after adsorption. These processes include the sputtering of surface species by energetic ions, diffusion of adsorbed radicals on the surface, the incorporation of radicals into the film, the desorption of radicals from the surface, and the elimination of hydrogen from the film by cross-linking between Si—H bonds in the near surface layers of the film. Gas phase-surface reactions are also simulated by including reactions between the impinging flux and the surface lattice species when nonsticking radicals strike the surface. For the results discussed here, we typically modeled the growth of a square patch of *a*-Si:H approximately 100–250 Å on a side having up to 1000 layers or a thickness of 2000–3000 Å. Periodic boundary conditions are used for the lateral dimensions of the film. In the discussion that follows, the term "site" denotes the *x*-*y* coordinate of a position on the film as viewed normally from the plasma. The term "lattice point" denotes the position of a particular atom or void in the film below a given site. There are many lattice points stacked vertically at each site.

The simulation proceeds schematically as follows. A flux of radicals is directed towards the surface, isotropically for neutrals and vertically for ions. The identity of the individual radical and the local morphology of the impingement site determines whether the radical adsorbs, sputters, bonds, or chemically reacts with the surface. An adsorbed, but nonbonded, radical may diffuse on the surface until encountering an activated site (i.e., a dangling bond, $\equiv$Si—•) at which time it bonds, a process which constitutes film growth. SiH_n radicals which bond to the film, may later interconnect with adjacent surface species to form the amorphous network. Cross-linking may occur between both nearest and next nearest neighbors, the latter possibly resulting in the formation of voids. Adsorbed species exceeding a specified residence time without bonding to the film may desorb, thereby enabling calculation of a sticking coefficient. By specifying characteristic frequencies for each process, the rate of occurrence of a particular event is determined relative to the rate of arrival of radicals on the surface. The model then proceeds as an effective integration in time of the equation of motions of each particle in the simulation.

An important feature of the model is the categorization of lattice points as being either in the near surface layer or in the bulk film. Since we desire to simulate volumes of *a*-Si:H films having 10^6–10^7 individual lattice points, it is not computationally practical to retain statistical information for each point. The model instead retains statistics for each lattice point in the near surface layer at each site. The near surface layer is typically 5–20 atoms deep. When a radical bonds to the surface at the top of the near layer, the lattice point at the bottom of the near layer is removed and its statistical information added to the average values for the bulk film. Although the near surface layers at each site are only 5–20 layers thick, the height of film at adjacent sites may differ by an arbitrary amount. Therefore, the rms difference in height (or roughness) of the film may exceed the near surface layer thickness.

A. Lattice points and site heights

Lattice points in the near surface layers are classified as being either unoccupied or occupied by a silicon atom. An occupied site is identified by its coordination partners. For example a point identified as SSSS denotes occupation by a silicon atom having four other Si atoms as coordination partners. A point identified as SSHD has two Si atoms and an H atom as coordination partners, and a dangling bond. Lattice points at a particular site which are unoccupied and buried beneath an occupied point are denoted as a void. The fraction of voids beneath the surface layer is therefore an indication of the porosity of the film. The topmost occupied lattice point is the surface of the film at that site. The average thickness of the film is then the average of the topmost heights for each site. The roughness of the film is the rms deviation of the thickness of the film from its average value.

B. Radical fluxes

The flux of neutral radicals incident on the surface may consist of an arbitrary mix of SiH_n $(0 \leqslant n \leqslant 3)$ or H. We do not presently consider disilane radicals. The flux of ions is assumed to consist of only a single generic charged species. The distribution of radicals is either specified as a part of a parametric survey, or is obtained from the results of the electron kinetics and plasma chemistry model described in Ref. 6. The time interval between impingement of a neutral radical from the plasma onto the surface is

$$\Delta t_R = (\Phi L^2)^{-1}, \tag{1}$$

where Φ is the total neutral radical flux and L is the physical length of the square of film we are simulating. The length is based on the width, in number of sites, of the lattice assuming an average lattice constant of 2.5 Å. For every Δt_R during the simulation a radical is directed towards the surface based on selection of a random number r $(0 < r \leqslant 1)$. The

particular radical which is directed towards the surface is that radical satisfying

$$F_{i-1} < r \leqslant F_i, \quad F_i = \sum_{j<i} f_j, \tag{2}$$

where f_i is the mole fraction of radical i in the flux of radicals incident on the surface. A similarly defined timer increment, Δt_I, for the ion flux determines the frequency with which ions are directed towards the surface.

The site on the surface (x_i, y_i) at which the selected radical impacts is randomly selected by use of two additional random numbers: $x_i = r_1 L$, $y_i = r_2 L$. The particular site is constrained in the following fashion. Assuming that the neutral radical flux is incident isotropically onto the surface, the probability that a radical impacts in a deep well (resulting from surface roughness) is small. The local morphology of the selected site is therefore inspected to determine whether the site sits at the bottom of a well. A well is defined as a site which is lower than the height of its nearest neighbor sites by an amount greater than or equal to the near surface layer. If this is the case, the radical which would have otherwise impacted in the well is placed on the surface site adjacent to the well. Assuming that ions are incident vertically, they may impact on any site including those in wells.

C. Selection criteria for plasma-surface reactions

The surface lattice points at any site may be classified as inert, passivated, or activated. An inert surface site is occupied by a silicon atom fully coordinated to other silicon atoms (i.e., SSSS). A passivated surface site is occupied by a silicon atom having at least one Si—H bond and no dangling bonds (e.g., SSHH) whereas an activated surface site is occupied by a silicon atom having at least one dangling bond (e.g., SSSD). All neutral silane radicals incident on an inert site are assumed to adsorb onto the surface. All neutral silane radicals incident on an activated site may directly incorporate into the lattice; for example,

$$SiH_2(g) + SSSD \rightarrow SSSS \rightarrow SHHD, \tag{3}$$

where (g) denotes a gas phase species.

Neutral silane radicals SiH_n, $n \leqslant 2$, may also incorporate into passivated sites by displacing a hydrogen atom from the surface species, a process which is nearly thermoneutral. For example,

$$SiH(g) + SSSH \rightarrow SSSS + SHHD. \tag{4}$$

SiH_n radicals with $n \leqslant 2$ therefore effectively have sticking coefficients of near unity unless later sputtered off the surface. In the model, silyl radicals (SiH_3) may only incorporate into an active surface site and therefore most often move directly into an adsorbed state since the fractional surface density of active sites is small. This condition is important in determining the surface properties since the mole fraction of SiH_3 radicals in the incident flux is typically $\geqslant 0.9$ for plasma conditions which result in device quality films.

The rate of generation and passivation of surface sites is important in two respects. First, the removal of hydrogen from the surface is important in the accounting of the total amount of hydrogen in the film and in determining the characteristics of the hydrogen rich surface layers. Second, the net rate of generation of dangling bonds on the surface by removing passivating H atoms in part determine the sticking coefficient for SiH_3 radicals since this radical requires an activated surface site for incorporation.

New passivated and active surface sites are continually being generated by radicals which incorporate into the film and constitute the new surface species at that site. Nonsticking radicals, molecules, and ions from the plasma may also react with the surface species to generate activated sites. Specifically, in the model we assume that an H atom (in the incident flux) landing on an active site passivates the dangling bond, whereas H atoms landing on a passivated site extract a hydrogen thereby etching the surface. For example,

$$H(g) + SSSD \rightarrow SSSH, \tag{5}$$

$$H(g) + SSSH \rightarrow SSSD + H_2(g). \tag{6}$$

The latter process is analogous to the gas phase hydrogen abstraction reaction,

$$H + SiH_4 \rightarrow SiH_3 + H_2. \tag{7}$$

The analogous reactions to Eqs. (5) and (6) may also occur with SiH_4 as the reactant instead of H. The former reaction,

$$SiH_4(g) + SSSD \rightarrow SSSH + SiH_3(g), \tag{8}$$

may be important since the flux of SiH_4 striking the surface is large compared to that for H. The etching reaction,

$$SiH_4(g) + SSSH \rightarrow SSSD + SiH_3(g) + H_2(g), \tag{9}$$

is not likely to be rapid since it is endothermic by approximately 1.9 kcal/mole.[11] Nevertheless, as will be discussed in Sec. IV, the net rate of passivation of the surface by SiH_4 is important in accounting for film properties.

Dangling bonds may also be generated by sputtering off the passivating H atom by ion impact and by sputtering of loosely adhered silicon containing surface species, for example,

$$M^+(g) + SSSH \rightarrow M^+(g) + SSSD + H(g). \tag{10}$$

The model ignores the direct contribution of ion impact to the densification of the film, as addressed by Mueller[12] and by Drevillon.[13] The precise mechanism for hydrogen removal by ion impact is not specified in the model, though it is assumed to be a combination of sputtering and thermal spiking. In the simulation, a maximum number of H atoms is specified, typically ten, that may be removed from passivated bonds per incident ion subject to the availability of ≡Si—H bonds in the vicinity of the ion impact. In practice, the average number removed per incident ion is less than ten due to this requirement.

Ion impact may also sputter off loosely adhered SiH_n groups on the surface, a process which has been described as "scouring" of the surface.[14] Typically, these groups are the terminus of polymeric chains which are not presently simulated in this model. To investigate the importance of this process, we defined loosely adhered SiH_n groups as species on the surface which have only one silicon atom as a coordination partner (i.e., SHHH, SHHD, SHDD, SDDD). We then included the process, for example,

$$M^+(g) + (SSSS\text{-}SHHH) \rightarrow M^+ + SSSD + SiH_3(g) \tag{11}$$

in the model. The importance of this process is discussed in Sec. IV.

D. Surface diffusion and reactions

During the simulation, adsorbed radicals on the surface, principally SiH_3, diffuse from surface site to surface site. Adsorbed radicals are moved from their current surface site with each increment of the global timer. The direction of the move in the plane of the surface (one of eight directions including nearest and next nearest neighbors) is determined by choice of a random number. An adsorbed radical is allowed to make a specified number of such moves before being removed from the surface; that is, being desorbed. The specified number of moves is an input parameter chosen to give a reasonable sticking coefficient. Under conditions which experimentally yield high quality films, allowing ten such moves for SiH_3 results in a sticking coefficient of 0.05–0.25, in fair agreement with recent measurements.[15,16]

The diffusive motion of the adsorbed radical is constrained in the following manner. The height of the film at a particular site is h. When an adsorbed radical is moved, we define the height of the film at the initial site as h_i and the height of the film at the site to which the adsorbed radical is chosen to move as h_f. Moves with $h_i \geqslant h_f$ are allowed; that is the adsorbed radical is allowed to make a lateral move or fall onto a site of lower height. Moves with $h_i < h_f$ are not allowed; that is the adsorbed radical is not allowed to climb to a higher surface site. An adsorbed species may be trapped in a well as a result of a move. A trapped radical is one which does not move from a surface site for the maximum number of attempted moves. In this case the model assumes that the radical is permanently trapped and will eventually bond at that location. It is therefore bonded in place and, if necessary, H_2 is eliminated.

When an adsorbed radical moves over a new surface site, it may bond to the occupying Si atom and incorporate into the film in the same manner as described above for neutral radicals incident from the plasma. An adsorbed radical which does not bond to the surface site beneath it is moved again on the next cycle. When an adsorbed radical moves to a surface site where the height of the film at an adjacent site is higher than its present location these are additional considerations. Under those conditions, as well as when the radical attempts a move with $h_f > h_i$, the adsorbed radical may bond with the lattice atom having the same height at the adjacent site. This adjacent lattice atom is buried beneath its own surface site and constitutes part of the near surface layer for that site.

E. Cross-linking, interconnection, and hydrogen elimination

Cross-linking is the process whereby ≡Si—• (e.g., SSSD) and ≡Si—H (e.g., SSSH) configurations, bond, and form the amorphous network of the film. Cross-linking is also an important process for removing hydrogen previously incorporated into the lattice. Cross-linking may occur between silicon atoms in adjacent sites having dangling bonds, for example,

$$\text{SSSD} + \text{SSSD} \rightarrow \text{SSSS} + \text{SSSS}, \tag{12}$$

or between silicon atoms in adjacent sites having passivated bonds, for example,

$$\text{SSSH} + \text{SSSH} \rightarrow \text{SSSS} + \text{SSSS} + \text{H}_2(g). \tag{13}$$

The former process is exothermic. The latter process, though being endothermic, is believed to be largely responsible for eliminating hydrogen from the film. An activation energy of 1.35 kcal/mole has been assigned to this process by observing hydrogen content as a function of substrate temperature.[17] Cross-linking may occur between ≡Si—H configurations topmost on the surface and those buried beneath the surface but exposed on a sidewall, a process which constitutes film densification.

Cross-linking, interconnection, and hydrogen elimination are simulated in the following fashion in the model. A characteristic site examination frequency for nearest neighbors, ν_n, and for next nearest neighbors, ν_{nn} are specified. These frequencies yield intervals, $\Delta t_n = 1/\nu_n$, which specify the average time between inspecting adjacent lattice points. After Δt_n has elapsed at a particular lattice point, a survey of nearest neighbor lattice points is made. The nearest neighbor lattice points are the ≡Si—• and ≡Si—H complexes within a lattice constant of the central point. If the central lattice point is a ≡Si—• complex, the survey consists of examining the nearest neighbor points in a random order searching for another ≡Si—• complex. A successful search results in an interconnection as shown in Eq. 12. If the central lattice point is a ≡Si—H complex, the survey searches for another ≡Si—H complex. If the search is successful, the choice of another random number determines whether there is enough thermal energy available for the endothermic process to take place. This is determined by having $-\ln(r) \geqslant \epsilon_3/T_s$, where r is a random number $(0,1)$, ϵ_a is the activation energy, and T_s is the substrate temperature. If these conditions are met, interconnection with hydrogen elimination occurs as shown in Eq. 13. The procedure described for nearest neighbor interconnection is also followed for next nearest neighbors, with the examination interval being $\Delta t_{nn} = 1/\nu_{nn}$.

F. Void formation

Cross-linking and interconnection with next nearest neighbors can result in the formation of voids (or porosity). The algorithm for these processes is identical to that described above for interconnection between nearest neighbors. The frequency of interconnection with next nearest neighbors, however, must be less than that for nearest neighbors as evidenced by the low porosity of films ($\lesssim 15\%$) which can be deposited. To account for this observation, a ratio of $\nu_n/\nu_{nn} \geqslant 50$ was typically used. As cross-linking with at most next nearest neighbors is allowed, the voids generated in the model are at most one lattice constant wide. They may, however, have either vertical or horizontal extents of up to many hundreds of lattice constants. In forming voids in this fashion, low porosity may occur in films which have an extremely rough surface, since it is not possible (in the model) to cross-link at greater distances than next nearest neighbors which would otherwise bridge roughness and form large voids. The large surface roughness, though, gives

the appearance of a porous near layer, and in measurements of surface roughness a void fraction is often cited based on the near layer roughness. Our definition of porosity are voids (vacant lattice points) below the topmost occupied lattice point at a site.

Occupied surface lattice points on both vertical and horizontal surfaces are usually passivated by hydrogen. Therefore, the formation of voids traps hydrogen below the surface. Our algorithms do not presently allow for evolution of hydrogen from subsurface sites and voids. Therefore the bulk hydrogen fractions for porous material (void fraction $>$ 10's of percent) are likely to be overestimated. This effect is discussed below.

III. SIMULATED PROPERTIES OF *a*-Si:H FILMS

In this section, we will discuss results obtained from our model for the simulation of the growth of hydrogenated amorphous silicon films from silane plasmas when the radical fluxes are specified as part of a parametric survey. In Sec. IV, we discuss results for when the radical fluxes are obtained from a companion model for the electron kinetics and plasma chemistry of discharges sustained in silane.[6]

Before beginning the parametric survey, we present a sample of a simulated surface of *a*-Si:H for typical plasma deposition parameters shown in Fig. 1. The radical fluxes for this case were obtained from the electron kinetics and plasma chemistry model. The discharge conditions are a silane pressure of 250 mTorr, substrate temperature of 500 K, and power deposition of 100 mW cm^{-3}. The total monosilane radical flux incident on the substrate is 2.5×10^{16} cm^{-2} s^{-1} in the ratio of $SiH_3/SiH_2/SiH/H = 0.93/0.0064/1.8\times10^{-4}/0.06$. The total ion flux incident on the surface is 1.3×10^{14} cm^{-2} s^{-1} and at most ten surface sites may be activated per incident ion. The frequencies for examination of nearest and next nearest neighbors are $\nu_n = 3.9$ s^{-1} and $\nu_{nn} = 8\times10^{-2}$ s^{-1}, respectively. The calculated deposition rate from the model using these parameters is 4.5 Å s^{-1}. The hydrogen fraction of the simulated film is $f_H = 12\%$, and the ratio of hydride/dihydride bonds in the bulk material is 2.1, which does not include the hydrogen rich surface layers. By summing the SiH_3 flux incident onto the surface and comparing the fluence to the amount of SiH_3 desorbing, we obtain a sticking coefficient for SiH_3 of $\sim$0.12. The calculated surface roughness (the rms deviation from the average film height of 750 Å) is approximately 20 Å. All of these parameters are in good agreeement with experimental results for device quality films grown by PECVD.[1] The qualitative appearance of the surface agrees well with recent scanning tunneling microscopy measurements of the surface of plasma deposited *a*-Si:H films.[18] Our predicted spin densities are fractionally large (a few times 10^{-4}, or ≈ 5–6×10^{18} cm^{-3}) for films which otherwise have good properties. Desirable spin densities are typically $\lesssim 10^{16}$ cm^{3}.[1] We interpret this discrepancy as there being thermal structural relaxation of the Si network *after* burial of the surface species which reduces the spin density,[1] a process we do not include in the model.

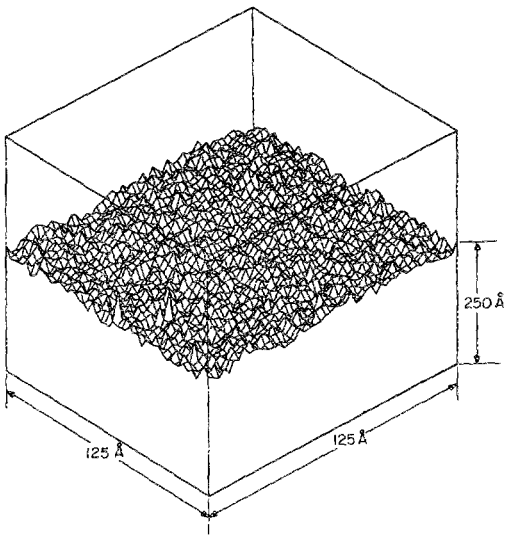

FIG. 1. Simulated surface of an *a*-Si:H film, being relatively smooth, deposited from a pure silane discharge (250 mTorr, power = 100 mW cm^{-3}). The film (area 125×125 Å^2) has an average thickness of 750 Å with an rms surface roughness of 20 Å.

A. Surface roughness

The surface roughness of *a*-Si:H films is important with respect to their use in thin-film devices and in multilayer structures where the lattice period may be comparable to the surface roughness.[19] Works by Knights,[20] Tsai *et al.*,[21] Collins and Cayese,[22–24] and Collins and Pawlowski[25] have resulted in a qualitative understanding of the origin and scaling of surface roughness. In summary, plasma conditions which have a predominance of silane radicals which have high sticking coefficients ($SiH_n, n\leqslant2$) generally result in rougher films and poor sidewall coverage. The low surface mobility for these radicals results in shadowing of precursor or random surface features and magnify their roughness. These conditions are found in low-pressure silane plasma ($<$ 100 mTorr) or diluted silane plasmas where the probability of radical scavanging reactions, exemplified by

$$SiH_2 + SiH_4 \rightarrow Si_2H_6^*, \tag{14}$$

is low. Deposition under these conditions resembles physical vapor deposition (PVD). It is generally believed that plasma conditions which result in radical fluxes dominated by SiH_3 result in smoother films and higher quality material, and resemble chemical vapor deposition (CVD).

To investigate the effect of adsorbant mobility on the roughness of *a*-Si:H films, we parameterized our model while varying the fraction of SiH_3 in an impinging flux consisting only of a mixture of SiH_2/SiH_3. Those results are shown in Fig. 2. We find that the surface roughness is relatively constant until the silyl fraction is less than 0.4, below which surface roughness increases markedly. As the growth rate is a function of SiH_3 fraction (see below) we performed our calculations for both constant growth rate and constant magnitude of the radical flux, and obtained similar roughnesses. The ion flux was kept constant throughout. These results imply that surface adsorbant mobility is most influential in determining the surface roughness. However, only moderate fractions of a highly mobile radical, such as SiH_3,

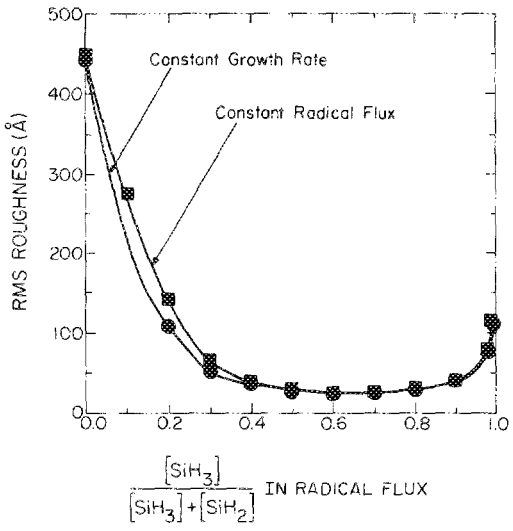

FIG. 2. rms surface roughness as a function of composition of the radical flux (SiH_3, SiH_2). PVD-like deposition resulting from a large SiH_2 fraction in the radical flux (>0.5) has a high surface roughness.

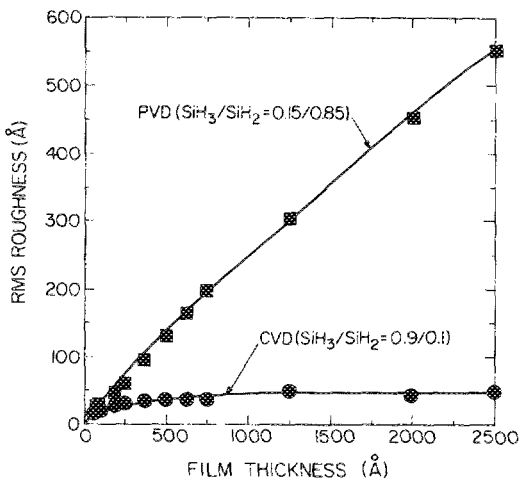

FIG. 3. rms surface roughness as a function of film height for PVD-like conditions ($SiH_3/SiH_2 = 0.15/0.85$ in incident radical flux) and CVD-like conditions ($SiH_3/SiH_2 = 0.9/0.1$). The rms roughness for PVD-like conditions increases with increasing film thickness due to shadowing effects. CVD-like conditions quickly reach an equilibrium when mobile adsorbed SiH_3 radicals on the surface fill in surface roughness at approximately its rate of generation.

is sufficient to fill in and smooth the surface. The sticking coefficient for SiH_3 is approximately 0.25 for these conditions. It appears, then, that the surface roughness generated by SiH_2 sticking in a PVD-like manner can be mitigated by having approximately $\gtrsim 0.1$ (0.5 flux fraction $\times 0.25$ sticking coefficient) of the deposition result from the higher mobility species, SiH_3.

Surface roughness is a function of film height, as well as deposition species. Collins and Cavese[22] found that for conditions dominated by PVD-like deposition surface roughness increased with increasing film height, whereas this dependence on film height was not as strong for CVD-like conditions. They found that roughness scales as $h^{0.33}$ for $0.2\ \mu\text{m} < h < 2\ \mu\text{m}$. Drevillon[13] has also found a correlation between growth rate and surface roughness. In that work, Drevillon viewed surface roughness as a porous overlayer on top of homogeneous bulk material.

We simulated *a*-Si:H films with different heights for CVD and PVD-like conditions by using incident radical fluxes of $SiH_3/SiH_2 = 0.9/0.1$ and 0.15/0.85, respectively. Our results are shown in Fig. 3. For PVD-like conditions surface roughness scales almost linearly with thickness. For CVD-like conditions surface roughness has only weak dependence on film thickness for thicknesses greater than 100 monolayers (about 250 Å). The poor scaling of surface roughness for PVD-like conditions (i.e., large ratios of SiH_2/SiH_3) results primarily from the shadowing effect of precursor or random roughness in the first few layers. Roughness increases with increasing thickness as the shadowing effect becomes more severe. This effect is likely exaggerated in our simulation by not including densification by ion impact and interconnection with more than second nearest neighbors (see below) though the roughness must clearly be greater than for the CVD-like conditions. For CVD-like conditions, a quasiequilibrium is reached between shadowing and the "filling" effect of mobile surface species.

For CVD-like film growth, the deposition species with a high surface mobility, SiH_3, requires a finite residence time on the surface to fill in roughness. This residence time must be sufficient to allow the mobile radicals to diffuse a distance approximately equal to the transverse dimension of the surface roughness. One would then expect that the surface roughness would increase with increasing deposition rate as the average residence time of mobile species on the surface decreases. In simulating films for CVD-like conditions, though, we find only a weak dependence of surface roughness on growth rate, as shown in Fig. 4.

B. Hydride/dihydride ratio

The ratio of buried hydride to dihydride configurations in *a*-Si:H films is also an indication of film quality, with bet-

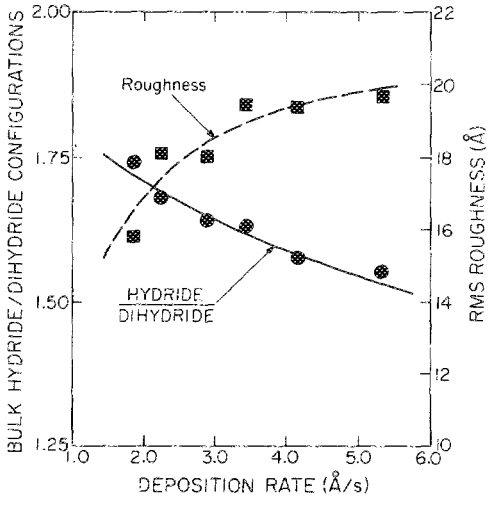

FIG. 4. Film properties as a function of film deposition rate; rms surface roughness and the ratio of buried hydride/dihydride configurations. The composition of the incident flux ($SiH_3/SiH_2 = 0.9/0.1$) was kept constant for all cases while the magnitude of the flux was varied. The average film thickness for all cases was 750 Å.

ter films (e.g., higher conductivity) having large (SSSH)/(SSHH) bond ratios.[26] In our simulations, this ratio decreases with increasing growth rate as shown in Fig. 4. Slower growth rates allow longer residence times of SSHH configurations on the surface, and therefore there is more opportunity for interconnection and hydrogen elimination which increases the hydride/dihydride ratio. Many of the dihydride configurations are contained in voids which, in our model, do not further interconnect (see below). Therefore the dihydride density may be overestimated. Low growth rates then appear to produce better material based on both roughness and hydride/dihydride ratio criteria.

C. Hydrogen fraction and porosity

Before discussing the relationship between hydrogen fraction and porosity, we are careful here to differentiate between surface roughness and voids. The former is an rms deviation of the surface height. The latter is the fraction of unoccupied lattice sites below the surface and is thus a measure of film porosity. We have therefore defined the term porosity to mean a true volumetric defect density. In the literature, the term porosity is often used to describe a defect density based on mean film thickness which includes surface roughness. For example, the (volumetric) void fraction of a typical film is 10%–20%. A defect density based on mean film thickness, defined as

$$R_a = (\text{average roughness})/(\text{mean film height}), \quad (15)$$

would add an additional defect density level of about 5% for a film having a roughness of 20 Å and height of 400 Å.

The atomic fraction of hydrogen in a-Si:H films, f_H, is of interest with respect to its effect on electronic properties, such as the optical band gap and photoconductivity. It is generally observed that f_H increases with increasing deposition rate.[14,27,28] This dependence has been attributed to a "burial effect" where the shorter residence times of ≡Si—H configurations on the surface resulting from increasing growth rates reduce the probability for cross-linking and hydrogen elimination. We found a similar dependence of hydrogen fraction on growth rate, as shown in Fig. 5; that is f_H increases with increasing growth rate. When we do not allow void creation, the same general dependence of f_H on growth rate is obtained, however the value of f_H is lower at slow growth rates. The increase in f_H at low growth rates correlates directly with an increase in the porosity of the film with decreasing growth rate, also shown in Fig. 5. This correlation between voids and hydrogen fraction has been made experimentally for both a-Si:H films,[14,29] and a-Ge:H films.[30] We find that large amounts of hydrogen are being trapped in voids as a result of the sidewalls being passivated by H atoms.

The increase in void fraction we predict at low deposition rates is typically not observed. Void fractions are either constant with growth rate or tend to increase with increasing growth rates under some conditions.[28] Mathematically, our result is a consequence of the fact that interconnection with next nearest neighbors occurs at a fixed rate, so slower growth implies more void formation. These conditions imply that ion impact densification and heating

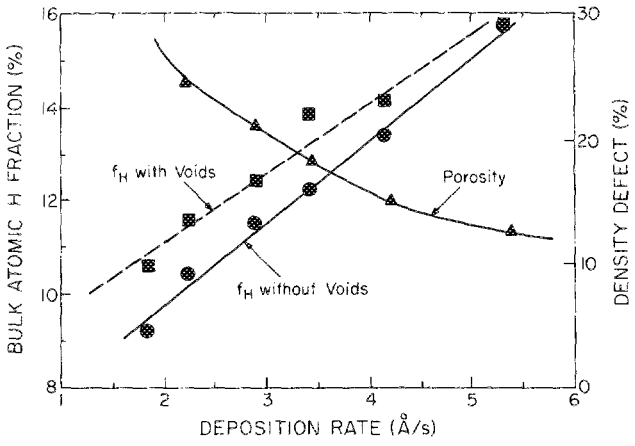

FIG. 5. The atomic hydrogen fraction and density defect due to porosity as a function of growth rate for the deposition conditions described in Fig. 4. The increase in hydrogen content at low growth rate for simulations where voids are created results from hydrogen being trapped in subsurface voids. The effect may be magnified by the model, which does not allow hydrogen evolution from voids after burial.

of the film, both of which will evolve hydrogen and close voids *after* burial, must be important.

The average void sizes obtained in our simulations are approximately 20–40 Å^3. We find that the atomic hydrogen content increases, and the ratio of hydride to dihydride configurations decreases, as the average void size increases. (See Fig. 6.) This correlation suggests that dihydride configurations are more likely to be found in voids, and by implication hydride configurations are more uniformly distributed. These predictions agree with the results of Reimer, Vaughan, and Knights[14] who, using NMR methods, were able to differentiate between isolated monohydride and grouped dihydride configurations in a-Si:H. Since films that have high monohydride fractions typically have better electrical properties, films having small void sizes should similarly have better properties.

The average void sizes in Fig. 6 are small, < 40 Å^3, and have equivalent spherical diameters of 3.5–4.0 Å. The distribution of voids is compact, with the relative density falling to $< 10^{-4}$ for voids having volumes of greater than a few hundred Å^3 (see Fig. 7). Beyond this size, the distribution

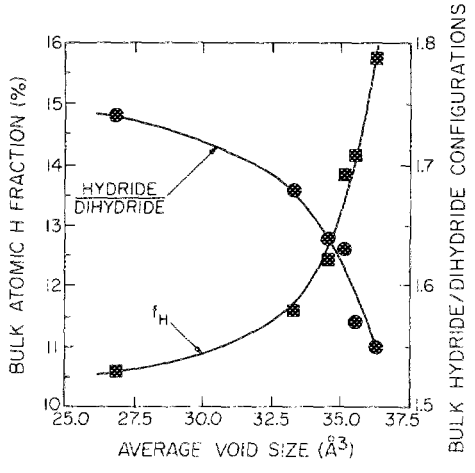

FIG. 6. Hydrogen content and hydride/dihydride ratio of a-Si:H as a function of average void size.

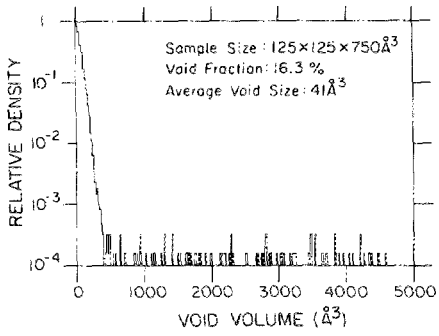

FIG. 7. Fractional distribution of voids as a function of void size. The average void volume is 40.9 Å^3 and the total void fraction is 16.3%. The sample size for this case is $125\times125\times750$ Å^{-3}.

has a long tail which extends to larger volumes. There are infrequent occurrences of voids having volumes greater than many thousand Å^3. These large voids tend to be long fissures, more often vertical than horizontal. For comparison, though, their equivalent spherical diameters are $\leqslant$20–25 Å.

Void fractions, or porosity, tend to be constant for films $>$750-Å thick and for deposition conditions for which SiH_3 is the predominant deposition radical, as shown in Fig. 8. For the cases shown, the void fraction of PVD-like depositions is less than that for CVD-like conditions when only subsurface porosity is considered. The porosity of the PVD-like material may be artificially low since the model limits void formation to those created by cross-linking with next nearest neighbors, which as described above, is not able to bridge over large roughness and create large voids. Cross-linking or bridging gaps across more than one lattice point is

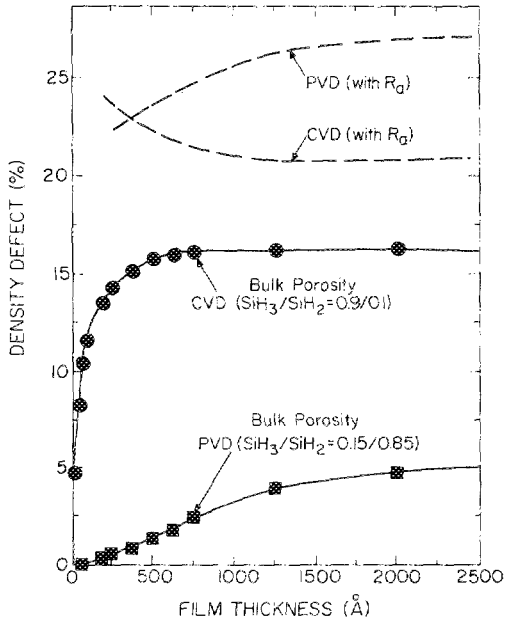

FIG. 8. Density defect as a function of film thickness. The simulated deposition conditions are the same as for Fig. 3. The solid lines denote bulk porosity. The predicted values for PVD-like conditions may be artificially low due to the assumption in the model that cross-linking can take place with at most next nearest neighbors. When the effect of surface roughness (R_a, dashed lines) is included, PVD films have a larger density defect than CVD-like films.

required for PVD-like deposition have a higher porosity than CVD-like conditions. When including the apparent density defect due to surface roughness, as given by R_a in Eq. 15, the defect density of the PVD-like films exceeds that of PVD-like films as shown in Fig. 8. The majority of density defect for thin PVD-like films ($<$2000 Å) can be attributed to surface roughness.

D. Hydrogen rich surface layers

The growth mechanism for *a*-Si:H films suggested by Gallagher implies that both lateral and vertical surfaces of the film are saturated by $\equiv$Si—H configurations.[5] This mechanism then requires that there be a hydrogen rich layer at the surface whose local depth is indicative of the depth of active growth, and whose average depth is approximately the surface roughness. Measurements of hydrogen evolution by post deposition sputtering of *a*-Si:H films have shown this layer to be 5 layers thick at room temperature, and a monolayer $>$500 K.[31] Simulations of film growth by Gleason *et al.* indicated that the active layer is 1.0–2.5 atoms deep[10] not including surface roughness. To account for the effect of this active layer on f_H, Gleason gives the expression $f_H = N_b f_b + N_s f_s$, where the subscripts denote bulk material b or surface layer material s, N is the fraction of atoms in a particular region, and f_i is the hydrogen fraction in region i. From our simulations we find that f_s is 0.5–2.0 depending on conditions. The local thickness of the hydrogen rich active region in our model is $<$4–5 layers as our computed hydrogen fractions are insensitive to the depth of our near layer for values $\gtrsim$5.

Extending this logic, the hydrogen content of the film should also scale proportionally to $\Delta h/h$, where Δh is the surface roughness, since more roughness provides more exposed surfaces which are passivated by H atoms. Since the ratio $\Delta h/h$ decreases with increasing film thickness, one would expect that the hydrogen content of thin films to be higher than that of thick films. Simulated hydrogen content as a function of film thickness is shown in Fig. 9. In very thin films (less than a few hundred Å's) f_H approaches 50%

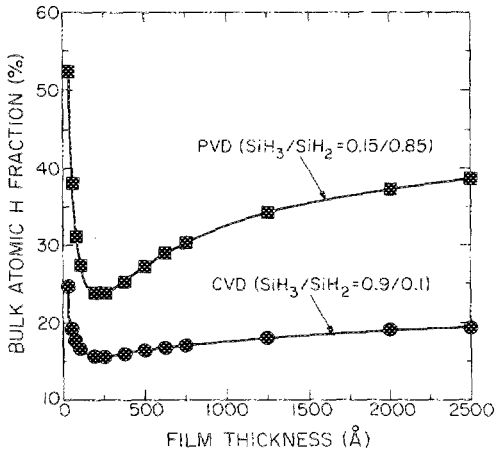

FIG. 9. Atomic hydrogen fraction, f_H as a function of film height for the same deposition conditions as used in Fig. 3. Thin films have higher f_H since a larger fraction of their atoms are contained in the hydrogen rich near surface layer.

since the exposed surface areas contain a significant fraction of all atoms in the lattice. For moderately rough films, we have found that up to 30% (roughness 40 Å, height 750 Å) of the total atomic hydrogen present in the films may be in the near layer region and within ~25 Å of the average surface. PVD-like conditions result in a higher hydrogen fraction due to their higher growth rate and larger surface roughness.

IV. *a*-Si:H FILMS FROM Ar/SiH_4 PLASMAS

It has generally been observed that the properties of *a*-Si:H films degrade upon dilution of the input silane gas with argon. The films become rougher,[22] begin growing with a columnar structure,[32] and the fraction of hydrogen found in voids or polyhydride configurations increases.[14] Concurrently, deposition rate and hydrogen fraction increase.[29] To simulate *a*-Si:H films using realistic deposition parameters, we computed radical fluxes using the plasma chemistry model described in Ref. 6 for a parallel plate rf PECVD reactor. The deposition conditions were 250 mTorr gas pressure and a substrate temperature of 500 K with an Ar/SiH_4 gas mixture. The power deposition was varied about 50 mW cm^{-3} in order to give the same flux of silane radicals onto the surface.

Computed flux characteristics are shown in Fig. 10(a) as a function of silane fraction in argon. As the mixture is diluted with argon, the ratio of SiH_3/SiH_2 in the incident flux decreases, and the ratio of the total ion flux to silane radical flux increases. The SiH_3/SiH_2 ratio decreases with argon dilution due to the lower net rates of radical scavenging reactions such as that in Eq. (14) and

$$H + SiH_4 \rightarrow SiH_3 + H_2, \tag{16}$$

both of which combine to increase the SiH_3/SiH_2 ratio. The ion to silane radical ratio increases due to there being a larger fraction of power coupled into argon which produces dominantly ions.

Simulated film properties for PECVD of *a*-Si:H in Ar/SiH_4 mixtures with a constant magnitude for the radical flux are shown in Fig. 10(b). We find that the bulk hydride/dihydride ratio decreases, deposition rate increases, and hydrogen fraction increases when pure silane is diluted with argon, in agreement with experiments.[14] The as-buried spin density also increases with argon dilution, in spite of increased hydrogenation of the film. This effect is likely a result of the higher rate of arrival of SiH_2 and higher growth rate which reduces the time for interconnection on the surface. Film roughness remains fairly constant for these conditions at ≈20 Å. This systematic agreement with experiment[14] was obtained by limiting the role of ions to sputtering loosely adhered SiH_n groups, and having the net rate of passivation of the surface be a constant. These results imply that the net rate of passivation by gas phase species is dominated by SiH_4 but rate limited by an activation energy barrier for the reverse process which produces dangling bonds. One should, therefore, find a more sensitive dependency of passivation on substrate temperature than silane partial pressure.

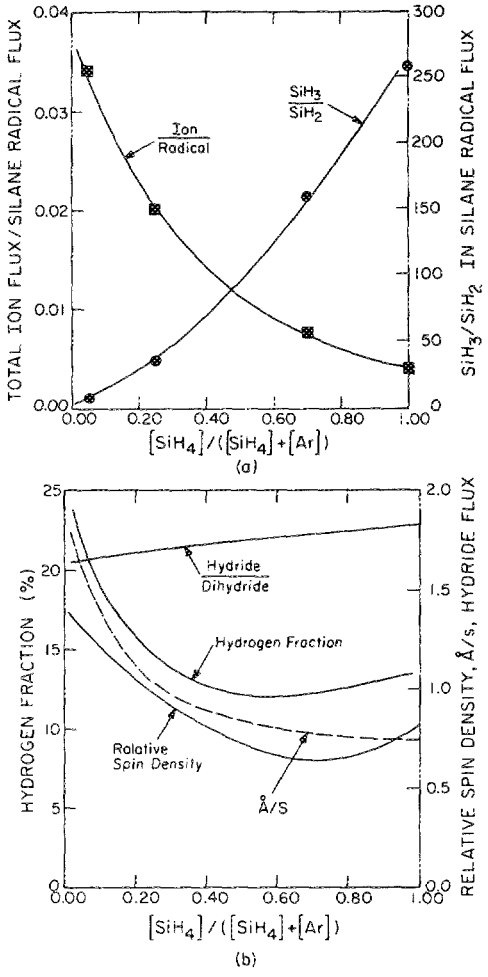

FIG. 10. (a) Computed parameters for the radical flux in SiH_4/Ar plasmas as obtained from the model described in Ref. 6. (b) Deposition rate, hydrogen fraction, as-buried spin density, and hydride/dihydride ratio for simulated *a*-Si:H films having a constant magnitude of silane radical flux for the conditions in (a). These results imply a degradation of film properties when diluting SiH_4 with argon.

V. CONCLUDING REMARKS

A model for the growth of *a*-Si:H thin films from silane plasmas has been presented. From the results of the model, we find that the physical properties of the film depend on both the relative fraction of the radicals in the incident flux and on the rate at which the radicals impinge on the surface. The roughness of the *a*-Si:H films depends most critically on the sticking coefficients of the impinging radicals, and secondarily on the deposition rate. We find that SiH_3 fractions of $> 50\%$ in the incident flux and deposition rates of < 3–4 Å/s produce smooth films (roughness < 20 Å). We also find a correlation between subsurface voids, hydrogen content, and high dihydride densities implying that hydrogen is trapped in voids when their passivated sidewalls are covered over. Subsurface evolution of the hydrogen trapped in these voids must likely take place in order to reduce the hydrogen fraction and void density of slowly growing films. In comparing our results to experiment, we find that passivation of dangling bonds on the surface is likely dominated by SiH_4, and not radical species. The observation that high quality

films are obtained in moderate pressure pure silane plasmas having low dissociation fraction is therefore partly explained by the following criteria. The silane pressure must be sufficiently high that insertion and abstraction reactions of radicals with the feedstock maintain a high ratio of SiH_3/SiH_2 in the radical flux. Low dissociation fractions are required to insure that passivation of the surface by SiH_4 is complete.

ACKNOWLEDGMENTS

The authors would like to acknowledge the support of the Army Research Office (Contract No. DAAG29-85-C-0031), under the direction of Dr. Andrew Crowson. The authors would also like to thank Dr. A. Gallagher, Dr. N. Mali, and B. Stafford for valuable discussions. Professor John Thornton, who died unexpectedly in November 1987, also contributed valuable insight to this work.

[1]K. Tanaka and A. Matsuda, Mater. Sci. Rep. **2**, 139 (1987).
[2]H. Fritzsche, Sol. Energy Mater. **3**, 447 (1980).
[3]F. Kampas, in *Semiconductors and Semimetals*, edited by J. I. Pankove (Academic, Orlando, 1984), Vol. 21A, p. 123.
[4]J. A. Thornton, in *Amorphous Metals and Semiconductors*, edited by P. Maasen and R. I. Jaffee (Pergamon, New York, 1986), pp. 299–314.
[5]A. Gallagher, J. Appl. Phys. **63**, 2406 (1988).
[6]M. J. Kushner, J. Appl. Phys. **63**, 2532 (1988).
[7]G. Turban, Y. Catherine, and B. Grolleau, Thin Solid Films **60**, 147 (1979).
[8]P. A. Longeway, R. D. Estes, and H. A. Weakliem, J. Phys. Chem. **88**, 73 (1984).
[9]K. Tachibana, in *Proceedings of the 8th Symposium on Ion Sources and Ion-Assisted Technology*, edited by T. Takagi (Institute of Electrical Engineering, Tokyo, Japan, 1984), p. 319.
[10]K. K. Gleason, K. S. Wang, M. K. Chen, and J. A. Reimer, J. Appl. Phys. **61**, 2866 (1987).
[11]B. H. Boo and P. B. Armentrout, J. Am. Chem. Soc. **109**, 3549 (1987).
[12]K. Mueller, J. Appl. Phys. **59**, 2803 (1986).
[13]B. Drevillon, Thin Solid Films **130**, 165 (1985).
[14]J. A. Reimer, R. W. Vaughan, and J. C. Knights, Phys. Rev. B **24**, 3360 (1981).
[15]J. Perrin and B. Allain, J. Non-Cryst. Solids **97/98**, 261 (1987).
[16]J. Perrin and T. Brockhuizen, Appl. Phys. Lett. **50**, 433 (1987).
[17]B. A. Scott, J. A. Reimer, and P. A. Longeway, J. Appl. Phys. **54**, 6853 (1983).
[18]R. Wiesendanger, L. Rosenthaler, H. R. Hidber, H.-J. Güntherodt, A. W. McKinnon, and W. E. Spear, J. Appl. Phys. **63**, 4515 (1988).
[19]M. Tsukude, S. Hata, Y. Kohda, S. Miyazaki, and M. Hirose, J. Non-Cryst. Solids **97/98**, 317 (1987).
[20]J. C. Knights, Mater. Res. Soc. Proc. **38**, 371 (1985).
[21]C. C. Tsai, J. C. Knights, G. Chang, and B. Wacker, J. Appl. Phys. **59**, 2998 (1986).
[22]R. W. Collins and J. M. Cavese, J. Appl. Phys. **61**, 1662 (1987).
[23]R. W. Collins and J. M. Cavese, J. Appl. Phys. **62**, 4146 (1987).
[24]R. W. Collins and J. M. Cavese, J. Non-Cryst. Solids **97** and **98**, 1439 (1987).
[25]R. W. Collins and A. Pawlowski, J. Appl. Phys. **59**, 1160 (1986).
[26]M. Pinarbasi, L. H. Chou, N. Maley, A. Myers, D. Leet, and J. A. Thornton, Superlattices and Microstructures **3**, 331 (1987).
[27]R. C. Ross and J. Jalik, Jr., J. Appl. Phys. **55**, 3785 (1984).
[28]O. Kuboi, M. Hashimoto, Y. Yatsurugi, H. Nagai, M. Aratani, M. Yanokura, S. Hayashi, I. Kohno, and T. Nozaki, App. Phys. Lett. **45**, 543 (1984).
[29]S. Kumar, K. K. Pandya, and K. L. Chopra, J. Appl. Phys. **63**, 1497 (1988).
[30]J. R. Blanco, P. J. McMarr, K. Vedam, and R. C. Ross, J. Appl. Phys. **60**, 3724 (1986).
[31]G. H. Lin, J. R. Doyle, M. He, and A. Gallagher, J. Appl. Phys. **64**, 188 (1988).
[42]J. C. Knights and R. A. Lujan, Appl. Phys. Lett. **35**, 244 (1979).